



SYNTHESIS OF ANALCIME ZEOLITE FROM GLASS POWDER WASTE AND ALUMINIUM ANODIZING WASTE

Magalhães, L. F.^{a,1}, da Silva, G. R.^a, Henriques, A. B.^a, Silvestrini, J. V.^a, Chiste, M. C.^a

^a Department of Mining Engineering, Federal University of Minas Gerais, MG, Brazil

1 Corresponding author. Email address: lucianofmag@demin.ufmg.br

ABSTRACT

In the present study, a two-step hydrothermal synthesis (alkaline fusion followed by hydrothermal treatment) of high-purity analcime zeolite was carried out from the combination of glass powder and aluminum anodization waste, two industrial wastes generated in large quantities and that have an ideal chemical composition for this purpose. The results revealed the formation of pure analcime, reaching crystallinity of up to 75%, confirmed by XRD analyses, while SEM analysis showed the presence of trapezohedral particles, typical of analcime. The experimental conditions investigated also enabled the formation of other zeolites, such as Na-P1, cancrinite and sodalite, demonstrating that the combination of glass powder and aluminum anodizing mud can be used to obtain different zeolitic phases. From the results obtained, it is concluded that products with greater added value can be generated from materials that are originally discarded after their respective production cycles, which can contribute to sustainability in the aluminum and glass industries.

Keywords: analcime, zeolite, industrial residues, circular economy, hydrothermal synthesis

1. INTRODUCTION

Zeolites belong to the class of aluminosilicates, formed from the union of TO₄-type tetrahedrons, where T can be represented by the elements silicon and/or aluminium (1). The difference in valence between these two elements generates a crystal structure with an excess of negative electrical charge. During its formation, the electrical charge is counterbalanced by compensation cations, usually elements of the alkali or alkali earth metal family (2). Another peculiarity of these minerals is their microporous structure, which presents pores smaller than 20Å, consequently resulting

in a solid with a high surface area. The combination of these properties makes zeolites an attractive option for application as adsorbents (3,4), water softener (5), catalysts in the petrochemical industry (6), gas separation (7), medicine (8), civil construction, as an addition to Portland cement (9), and many others.

Despite the possibility of producing synthetic zeolites, the process is costly, especially due to the chemical reagents used as a source of silicon and aluminium. An alternative approach is to use raw materials with high silicon and aluminium content as precursors, adding economic benefits to the synthesis, which encouraged the search for low-cost precursor materials (10). Among the various industrial residues that can be used as sources of silicon and aluminium in the synthesis of analcime, glass powder waste (GPW) and aluminium anodizing waste (AAW) stand out for their chemical composition.

The glass powder is a silicon-rich waste generated during the cutting and polishing step in the production of glass pieces. It is estimated that the production of GPW accounts for approximately 5% of the total solid waste generated globally (11). The disposal of GPW in landfills has become a common activity, and due to the low biodegradability of glass, this practice is considered harmful to the environment (12). The electrochemical process responsible for the formation of an oxide layer on the surface of aluminium pieces, aiming at protection against corrosion is known as aluminium anodizing. It is estimated that for every 1 ton of aluminium treated by anodizing, 475 kg of anodizing waste is generated, consisting mostly of aluminium oxyhydroxide (39). After solid-liquid separation, this residue, considered non-toxic and non-inert, is disposed of in landfills, and because of the alkalinity of this waste, significantly contributes to environmental impact (14).

This research was conducted using the combination of GPW and AAW as precursors, aiming at the production of single-phase analcime zeolite. The Plackett Burman statistic design was applied to evaluate which synthesis variables investigated in this study present greater statistical relevance, enabling future optimization.

2. MATERIALS AND METHODS

2.1. Precursor Materials

Glass powder waste (GPW) and aluminium anodizing waste (AAW) were used as precursor materials as sources of silicon and aluminium, respectively, being supplied by Bend Glass Comércio e Indústria LTDA and Akrominas - Comércio de Alumínio LTDA, both located in Contagem (Minas Gerais, Brazil). The materials were oven-dried at 100 °C for 48 h and deagglomerated in a porcelain ball mill for 30 min. As a source of alkali, sodium hydroxide in micropellets (reagent grade 98%) was used. During the synthesis, deionized water obtained from reverse osmosis filter (conductivity <1.5 µS.cm) was used, to avoid any ions that could interfere in the synthesis.

2.2. Materials characterization

The chemical composition of the GPW and AAW was determined via X-ray fluorescence (XRF) analysis using a Rayny EDX-720 Spectrometer (Shimadzu, US). The identification of crystalline phases in the samples of precursor materials was performed by X-ray diffraction (XRD) analysis, in an Empyrean X-ray Diffractometer (Malvern Panalytical, UK), operating with Cu k-alpha radiation (40 kV, 30 mA), 2θ ranging from 5 to 90°, at 0.06 °/s. The crystalline phases were identified using Match3! software, with Crystallography Open Database (revision. 184238). For synthesized analcime, the 2θ range was set from 3 to 50°, at 0.02 °/s step, since the characteristic peaks of zeolites occur at low 2θ angles. The crystalline phases were identified using Match3! software, followed by semi-quantification using the Rietveld method. The crystallographic patterns used for crystalline phase identification in synthesized analcime samples were obtained from the International Zeolite Association Database. The crystallinity determination was performed by measuring the ratio between the peak area and the total area in the sample diffractogram, according to Equation (1) (15).

$$\%crystallinity = \frac{\text{Sum of cristalline peaks area}}{\text{Total area}} * 100 \quad (1)$$

The size distribution of precursor materials was measured by a Laser Particle Analyzer 1064L (Cilas, FR). The samples were deagglomerated in an ultrasonic bath for 200 seconds. Scanning electron microscopy (SEM) was performed using a Quanta 200 FEI microscope (Thermofisher, US), with a resolution of 1.6 nm, operating with 10

to 15 kV. The samples underwent carbon metallization before analysis to provide good electric conductivity.

2.3. Zeolite synthesis

The synthesis of analcime zeolite from GPW and AAW was conducted in a 2-step process (alkaline fusion followed by hydrothermal synthesis). Initially, a given mass of GPW, AAW, and NaOH was measured on an analytical digital balance, hand-milled to homogenize the mixture, and then calcined in a porcelain crucible. The material resulting from the alkaline fusion was dissolved in deionized water and stirred for 1h. Then, 20 mL of the solution was transferred to a Teflon-lined stainless-steel autoclave, remaining in an oven for crystallization. At the end of the process, the solid obtained was filtered and washed several times until pH 9 was reached, to remove excess Na⁺ ions. Finally, the solid was oven-dried at 60°C for 24 h.

2.4. Plackett Burman statistic design

For the development of this research, 7 variables were combined in a 12-run non-geometric experimental design, as shown in Table 1. The crystallinity (%) and analcime content (%) in the products obtained from the synthesis were defined as response variables. The experimental design was conducted in duplicate, and the mean values of crystallinity (%) and analcime content (%) were taken.

Table 1 – Plackett Burman experimental design.

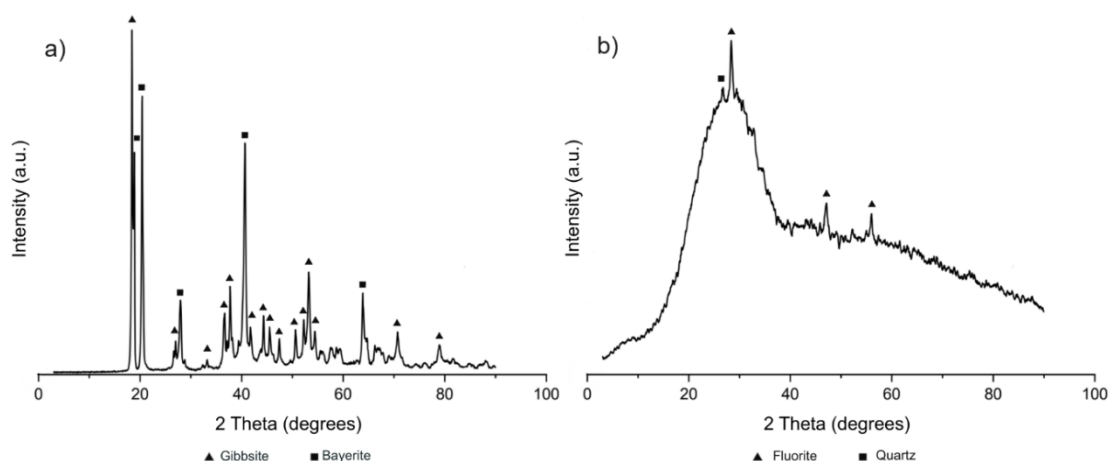
Test number	C _{temp}	C _{time}	SiO ₂ / Al ₂ O ₃	Na ₂ O / SiO ₂	H ₂ O / Na ₂ O	Cr _{temp}	Cr _{time}
1	700	2	8	15	200	110	24
2	500	3	8	6	200	90	24
3	700	3	2,5	6	300	110	24
4	700	3	2,5	6	200	110	4
5	700	2	2,5	15	300	90	24
6	500	2	8	6	300	110	24
7	500	2	2,5	15	200	110	24
8	500	3	8	15	300	110	4
9	700	2	8	6	300	90	4
10	500	3	2,5	15	300	90	4
11	700	3	8	15	200	90	4
12	500	2	2,5	6	200	90	4

3. RESULTS AND DISCUSSION

3.1. Characterization of GPW and AAW

Figure 1 shows the diffractograms obtained from the AAW and GPW samples from XRD analysis. The AAW sample (Figure 1a) exhibits the absence of an amorphous halo, and high-intensity peaks, revealing the crystalline nature of this material. The peaks observed can be assigned to gibbsite (α -Al(OH)₃, COD 9015976) and bayerite (β -Al(OH)₃, COD 1000061), isomorphous forms of aluminium hydroxide. The crystalline form of AAW implicates high chemical stability, which impairs the dissolution of the material, and consequently, limits the amount of Al³⁺ in the precursor gel. The GPW diffractogram reveals low-intensity peaks of fluorite (CaF₂, COD 9007064) and quartz (SiO₂, COD 1011097), and can be seen in the diffractogram the presence of an amorphous halo (Figure 1b), which characterizes GPW as an amorphous material. Even though amorphous materials can present high chemical reactivity, glass hardly solubilizes, impairing the liberation of Si⁴⁺ in the precursor gel. Since the two materials are insoluble in water, it is necessary to subject them to alkaline fusion. In this process, the materials are fused with an alkali reagent, e.g., sodium hydroxide, at temperatures ranging from 500 to 700°C. The products of this reaction are sodium aluminate and sodium silicate, both soluble species (16).

Figure 1 – X-ray diffractograms of AAW (a) and GPW (b).



The GPW and AAW chemical composition and size distribution are described in Table 2. AAW is mainly composed of aluminium and shows a low percentage of other contaminant elements. The high temperatures involved in the alkaline fusion can

volatilize these compounds and lead to the dehydration of aluminium hydroxides. The GPW is composed of silicon (70.6%) and calcium + sodium (approximately 22%), elements used in the glass fabrication process. The sodium present in GPW acts as a Na⁺ source, which can reduce the amount of NaOH needed in the synthesis. Table 2 also shows the size distribution of the GPW and AAW samples. The medium diameter (D_m) measured for GPW and AAW were 9.0 and 25.4 μm, respectively. The materials fineness is a consequence of its generation (abrasion and precipitation). It is not necessary to grind the material to obtain this size distribution (only to deagglomerate the materials after drying), which results in lower energy consumption. Another advantage is the materials fineness, enabling a more homogeneous mixture with the sodium hydroxide, which favours the chemical reactions in the alkali fusion step.

Table 2 – Chemical composition and particle size distribution of GPW and AAW

Chemical composition (%wt)	GPW	AAW
SiO ₂	70.6	0.2
Al ₂ O ₃	1.1	64.6
CaO	10.4	-
Cr ₂ O ₃	-	-
Fe ₂ O ₃	0.3	0.3
K ₂ O	0.2	-
MgO	0.8	-
MnO	-	-
Na ₂ O	11.9	1.1
P ₂ O ₅	0.3	-
TiO ₂	0.1	-
LOI	4.1	33.7
Particle size distribution (μm)		
D _m	9.0	25.4
D ₁₀	1.4	4.6
D ₅₀	7.8	25.2
D ₉₀	21.4	43.4

3.2. Main variables in the analcime synthesis

Table 3 summarizes the coefficients and effects obtained from the Plackett Burman statistic design on crystallinity (%) and analcime content (%). Crystallization time (Crtime) and temperature (Crtemp) are the variables with the greatest statistical significance (p-value 0.04 and 0.06, respectively) for analcime content (%), positively affecting the response. For crystallinity (%), Crtime and Crtemp were not considered significant (p-value 0.14 and 0.13, respectively) since the responses are higher than the 0.05 significance level. However, considering the effect values seen in Table 3, among all variables analyzed in this study, crystallinity (%) is positively affected by Crtime and Crtemp. As verified in Table 4, the tests reaching greater crystallinity are

those conducted at the high-level values of time and temperature. In tests conducted at a low level, the products obtained showed lower crystallinity, because the energy supplied is relatively low for the analcime to crystallize properly. At high-level temperatures and low-level time, crystallinity is also impaired, as nuclei begin to form, but there is not enough time for the crystals to grow (17).

The $\text{Na}_2\text{O}/\text{SiO}_2$ ratio shows greater influence for analcime content (%) (Effect 27.53) compared to crystallinity (%) (Effect 9.10), positively affecting both responses. The amount of Na^+ ions had a strong influence on crystallization, impairing analcime crystallization when present in low concentration in the precursor gel. In research verifying the influence of different mineralizing agents, the authors concluded that a low concentration of Na^+ prevents the crystallization of analcime (18).

The $\text{SiO}_2/\text{Al}_2\text{O}_3$ ratio is the variable that presented the lowest statistical relevance for crystallinity (%) (Effect -4.83) since a wide range of values allows the crystallization of several zeolitic phases, as verified in this study. However, the $\text{SiO}_2/\text{Al}_2\text{O}_3$ ratio possesses a small positive effect on the analcime content (%) response (2.63), since a specific range of $\text{SiO}_2/\text{Al}_2\text{O}_3$ is required for this zeolitic phase to crystallize. Consequently, for the synthesis of any zeolite, this is an important variable to be considered when seeking the production of a single-phase specific zeolite (15).

The $\text{H}_2\text{O}/\text{Na}_2\text{O}$ ratio has a negative effect on the analcime content (%) (Effect -8.15), although it affects crystallinity (%) more pronouncedly (Effect -11.34). In this case, increasing values of this variable negatively affect both responses. The greater amount of water in the system leads to a lower concentration of Na^+ ions in the precursor gel (19), which, as discussed earlier, inhibits the formation of analcime. In the case of crystallization, the greater dilution of the solution makes the monomers more difficult to nucleate, and consequently, reduces the crystal growth rate (20).

The calcination time (Ctime) and the calcination temperature (Ctemp) showed Effect 18.70 and 1.80, respectively, for analcime content (%), and Effect 6.53 and -6.88, respectively, for crystallinity (%). The melting point of sodium hydroxide is

observed at approximately 500°C, and the conversion of GPW and AAW into soluble Na-salts is possible at this temperature (21).

Table 3 – Summary of coefficients and effects on response variables for 95% confidence level.

Variables	Analcime content (%)				Crystallinity (%)			
	Effect	Coef	<i>t</i> -value	<i>p</i> -value	Effect	Coef	<i>t</i> -value	<i>p</i> -value
C _{temp}	1.80	0.90	0.15	0.89	-6.88	-3.44	-0.82	0.46
C _{time}	18.70	9.35	1.52	0.20	6.53	3.26	0.78	0.48
SiO ₂ /Al ₂ O ₃	2.63	1.32	0.21	0.84	-4.83	-2.42	-0.58	0.59
Na ₂ O/SiO ₂	27.53	13.77	2.24	0.01	9.10	4.55	1.09	0.34
H ₂ O/Na ₂ O	-8.15	-4.08	-0.66	0.54	-11.34	-5.67	-1.36	0.25
C _{temp}	36.08	18.04	2.93	0.04	15.77	7.89	1.89	0.13
C _{time}	32.67	16.33	2.65	0.06	15.26	7.63	1.83	0.14

3.3. Analcime characterization

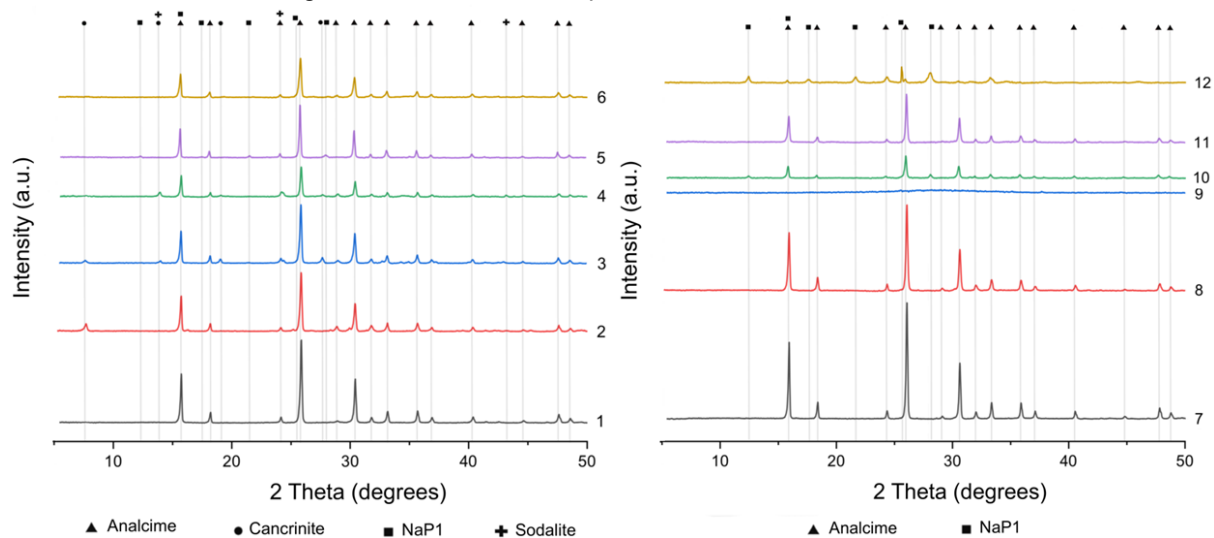
Figure 2 show the XRD results for the products obtained in all tests, and Table 4 summarizes the results of crystallinity and mineralogic composition obtained by Rietveld refinement in each test. The goal of synthesizing single-phase analcime zeolite was achieved in most tests, especially tests 1 and 7, and in addition to purity, the synthesized analcime showed high crystallinity, due to the absence of an amorphous halo. Analcime, cancrinite (Na₆CaCO₃[Al₆Si₆O₂₄].2H₂O, CAN framework), sodalite (Na₈Cl₂[Al₆Si₆O₂₄], SOD framework) and Na-P1 (Ca₄[Al₈Si₈O₃₂].16H₂O, GIS framework) are the phases competing during crystallization, making the definition of limits for the experimental variables of great importance to obtain single phase analcime zeolite. It is reported in the literature that the optimum crystallization time for analcime is approximately 24 h (22). Although the temperature was indicated to be set at 200 °C (23), in this research it was possible to obtain single phase analcime at 110 °C. According to the XRD results, the formation of Na-P1 zeolite was verified in tests 5, 10, and 12, which have lower crystallization temperature values. As verified by (24), the crystallization of GIS framework can be achieved at temperatures of 90°C, and above 100°C the formation of a mixture of GIS framework and analcime was verified, according to the results obtained in the present study. Despite the formation of two phases, due to the short crystallization time, in the aforementioned tests, the crystallinity observed was relatively low (24).

Table 4 – Crystallinity and phase composition of synthesized products

Test number	Crystallinity (%)	Analcime (%)	Cancrinite (%)	Sodalite (%)	Na-P1 (%)
1	74.9	100.0	0.0	0.0	0.0
2	74.5	85.2	14.9	0.0	0.0
3	72.0	93.0	7.1	0.0	0.0
4	61.9	92.6	0.0	7.5	0.0
5	65.8	97.2	0.0	0.0	2.9
6	65.5	100.0	0.0	0.0	0.0
7	75.4	100.0	0.0	0.0	0.0
8	65.9	100.0	0.0	0.0	0.0
9	12.2	0.0	0.0	0.0	0.0
10	52.8	62.7	0.0	0.0	37.3
11	60.7	100.0	0.0	0.0	0.0
12	54.8	24.0	0.0	0.0	76.0

According to the results shown in Table 4, the highest crystallinity was observed in test 7, and this sample was subjected to further characterization by scanning electron microscopy.

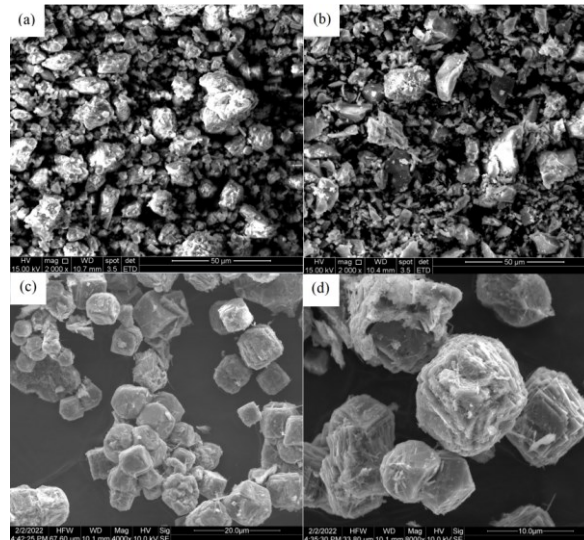
Figure 2 – XRD results of products obtained in tests 1 to 12



SEM images of the precursor materials and analcime are shown in Figure 3. The AAW particles (Figure 3a) present rough surfaces that may be related to the precipitation of $\text{Al}(\text{OH})_3$ in the formation by precipitation of the anodizing waste. As for GPW (Figure 3b), the cutting and polishing of glass pieces result in the formation of sharp-edged particles. Both materials exhibit a wide particle size distribution, consistent with the particle size analysis in terms of their D_{90} and D_{10} (1.4 and 21.4 μm , respectively, for GPW, 4.6 and 43.4 μm , respectively, for AAW). In contrast, visually,

analcime particles present a relatively uniform particle size distribution (Figure 3c), with particles of approximately 10 μm . In Figure 3d it can be visualized the presence of particles in the form of tetrahedrons, characteristic of analcime, and this morphology was verified in previous studies (24).

Figure 3 – SEM images of the precursor materials AAW (a) and GPW (b), and the synthesized analcime zeolite (c) and (d).



4. CONCLUSIONS

In this work, single-phase analcime with high crystallinity was synthesized from the combination of glass powder waste and aluminium anodizing waste. Due to precursor materials insolubility, a 2-step approach was used, i.e., alkaline fusion followed by hydrothermal synthesis. From the results obtained by the Plackett Burman statistic design, crystallization temperature and crystallization time were observed to be the variables with the greatest statistical relevance in the formation of analcime content (%), whereas alkaline fusion temperature and time presented the least relevance for analcime content (%) and crystallinity (%). The synthesized analcime obtained showed crystallinity up to 75%, although the results indicated that the optimization of the variables may lead to the formation of pure analcime with higher crystallinity. The results indicate that obtaining zeolites, especially analcime, for application in various industrial sectors is an alternative for the reuse of GPW and AAW, adding value to these residues, and contributing to sustainability and a circular economy.

Acknowledgements

The authors acknowledge Pró-Reitoria de Pesquisa (PRPq – Universidade Federal de Minas Gerais), CNPq, FAPEMIG, CAPES, and PROEX CAPES for their support of PPGEM.

REFERENCES

- (1) S. SIVALINGAM, S. SEN. Optimization of synthesis parameters and characterization of coal fly ash derived microporous zeolite X. *APPLIED SURFACE SCIENCE*, 455 (2018). <https://doi.org/10.1016/j.apsusc.2018.05.222>.
- (2) J.A.B.L.R. ALVES, E.R.S. DANTAS, S.B.C. PERGHER, D.M.A. MELO, M.A.F. MELO. Synthesis of high value-added zeolitic materials using glass powder residue as a silica source. *MATERIALS RESEARCH*, 17 (2013) <https://doi.org/10.1590/s1516-14392013005000191>.
- (3) J. CHEN, R. HUANG, H. OUYANG, G. YU, Y. LIANG, Q. ZHENG. Utilization of dredged river sediments to synthesize zeolite for Cd(II) removal from wastewater. *JOURNAL OF CLEANER PRODUCTION*, 320 (2021) <https://doi.org/10.1016/j.jclepro.2021.128861>.
- (4) L.F. DE MAGALHÃES, G.R. DA SILVA, A.E.C. PERES. Zeolite application in wastewater treatment. *ADSORPTION SCIENCE AND TECHNOLOGY*, 2022 (2022) <https://doi.org/10.1155/2022/4544104>.
- (5) A.M. CARDOSO, M.B. HORN, L.S. FERRET, C.M. AZEVEDO, M. PIRES. Integrated synthesis of zeolites 4A and Na-P1 using coal fly ash for application in the formulation of detergents and swine wastewater treatment. *JOURNAL OF HAZARDOUS MATERIALS*, 287 (2015) <https://doi.org/10.1016/j.jhazmat.2015.01.042>.
- (6) F. COLLINS, A. ROZHKOVSKAYA, J.G. OUTRAM, G.J. MILLAR. A critical review of water resources, synthesis, and applications for zeolite LTA. *MICROPOROUS MESOPOROUS MATERIALS*, 291 (2020) [10.1016/j.micromeso.2019.109667](https://doi.org/10.1016/j.micromeso.2019.109667).
- (7) N. KOSINOV, J. GASCON, F. KAPTEIJN, E.J.M. HENSEN. Recent developments in zeolite membranes for gas separation. *JOURNAL OF MEMBRANE SCIENCE*, 499 (2016) <https://doi.org/10.1016/j.memsci.2015.10.049>.
- (8) E. KHODAVERDI, H.A. SOLEIMANI, F. MOHAMMADPOUR, F. HADIZADEH. Synthetic zeolites as controlled-release delivery systems for anti-inflammatory drugs. *CHEMICAL BIOLOGY & DRUG DESIGN*, 87 (2016) <https://doi.org/10.1111/cbdd.12716>.
- (9) M. DAS, S.K. ADHIKARY, Z. RUDZIONIS. Effectiveness of fly ash, zeolite, and unburnt rice husk as a substitute of cement in concrete. *MATERIALS TODAY: PROCEEDINGS*, 61 (2022) <https://doi.org/10.1016/j.matpr.2021.09.005>.
- (10) T.A. VERESHCHAGINA, E.A. KUTIKHINA, L.A. SOLOVYOV, S.N. VERESHCHAGIN, E.V. MAZUROVA, Y.Y. CHERNYKH, A.G. ANSHITS. Synthesis and structure of analcime and analcime-zirconia composite derived from coal fly ash cenospheres. *MICROPOROUS MESOPOROUS MATERIALS*, 258 (2018) <https://doi.org/10.1016/j.micromeso.2017.09.011>.
- (11) S. DADSETAN, H. SIAD, M. LACHEMI, M. SAHMARAN. Evaluation of the tridymite formation as a technique for enhancing geopolymers based on glass waste. *JOURNAL OF CLEANER PRODUCTION*, 278 (2021) <https://doi.org/10.1016/j.jclepro.2020.123983>.
- (12) Y. DU, W. YANG, Y. GE, S. WANG, P. LIU. Thermal conductivity of cement paste containing waste glass powder, metakaolin and limestone as supplementary cementitious material. *JOURNAL OF CLEANER PRODUCTION*, 287 (2021) <https://doi.org/10.1016/j.jclepro.2020.125018>.
- (13) V. MYMRIN, D.E. PEDROSO, C. PEDROSO, K. ALEKSEEV, M.A. AVANCI, E. WINTER, L. CECHIN, P.H.B. ROLIM, A. IAROZINSKI, R.E. CATAI. Environmentally clean composites with hazardous aluminum anodizing sludge, concrete waste and lime production

- waste. JOURNAL OF CLEANER PRODUCTION, 174 (2018)
<https://doi.org/10.1016/j.jclepro.2017.10.299>.
- (14) M.T. SOUZA, L. SIMAO, O.R.K. MONTEDO, F. RAUPP PEREIRA, A.P.N. DE OLIVEIRA. Aluminum anodizing waste and its use: an overview of potential applications and market opportunities. WASTE MANAGEMENT, 84 (2019)
<https://doi.org/10.1016/j.wasman.2018.12.003>.
- (15) A. IQBAL, H. SATTAR, R. HAIDER, S. MUNIR. Synthesis and characterization of pure phase zeolite 4A from coal fly ash. JOURNAL OF CLEANER PRODUCTION., 219 (2019)
<https://doi.org/10.1016/j.jclepro.2019.02.066>.
- (16) S.Ş. AKIN, S.K. KIRDECILER, F. KAZANÇ, B. AKATA. Critical analysis of zeolite 4A synthesis through one-pot fusion hydrothermal treatment approach for class F fly ash. MICROPOROUS MESOPOROUS MATERIALS, 325 (2021)
<https://doi.org/10.1016/j.micromeso.2021.111338>.
- (17) Z. QIANG, X. SHEN, M. GUO, F. CHENG, M. ZHANG. A simple hydrothermal synthesis of zeolite X from bauxite tailings for highly efficient adsorbing CO₂ at room temperature. MICROPOROUS MESOPOROUS MATERIALS, 287 (2019)
<https://doi.org/10.1016/j.micromeso.2019.05.062>.
- (18) S.-X. BAI, L.-M. ZHOU, Z.-B. CHANG, C. ZHANG, M. CHU. Synthesis of Na-X zeolite from Longkou oil shale ash by alkaline fusion hydrothermal method. CARBON RESOURCES CONVERSION, 1 (2018) <https://doi.org/10.1016/j.crcon.2018.08.005>.
- (19) Y.-J. LIN, J.-C. CHEN. Resource recovery and valorization of waste incineration fly ash for the synthesis of zeolite and applications. JOURNAL OF ENVIRONMENTAL CHEMICAL ENGINEERING, 9 (2021) <https://doi.org/10.1016/j.jece.2021.106549>.
- (20) H. MORI. Extraction of silicon dioxide from waste colored glasses by alkali fusion using potassium hydroxide. JOURNAL OF MATERIALS SCIENCE, 38 (2003)
<https://doi.org/10.1023/A:1025100901693>.
- (21) A. JIMÉNEZ, A. MISOL, Á. MORATO, V. RIVES, M.A. VICENTE, A. GIL, J. Synthesis of pollucite and analcime zeolites by recovering aluminum from a saline slag. JOURNAL OF CLEANER PRODUCTION, 297 (2021) <https://doi.org/10.1016/j.jclepro.2021.126667>.
- (22) S. MINTOVA, N. BARRIER, Verified syntheses of zeolitic materials, 3 ed., Elsevier 2016.
- (23) AZIZI, S. N., DAGHHIGH, A. A., ABRISHAMKAS, M. Phase transformation of zeolite P to Y and analcime zeolites due to changing the time and temperature. JOURNAL OF SPECTROSCOPY, 2013. [dx.doi.org/10.1155/2013/428216](https://doi.org/10.1155/2013/428216)
- (24) R. VIGIL DE LA VILLA MENCÍA, E. GOITI, M. OCEJO, R.G. GIMÉNEZ. Synthesis of zeolite type analcime from industrial wastes. MICROPOROUS MESOPOROUS MATERIALS, 293 (2020) <https://doi.org/10.1016/j.micromeso.2019.109817>.